Acta of Bioengineering and Biomechanics
Vol. 24, No. 4, 2022

Original paper
DOI: 10.37190/ABB-02172-2022-05

Characteristic research of lower extremity injuries in elderly pedestrians during collisions

SEN XIAO[1, 2], LIDONG ZHANG[1], JINDONG WU[1], XINRAN LIU[3], XIAOANG LIU[1]*, HAO ZHANG[1]

[1] School of Mechanical Engineering, Hebei University of Technology, Tianjin, China.
[2] Tianjin Key Laboratory of Power Transmission and Safety Technology for New Energy Vehicles, Hebei University of Technology, Tianjin, China.
[3] China FAW Group Corporation,Changchun, China.

Purpose: The aim of this research is to study the trend of pedestrian lower extremity injuries during vehicle-pedestrian collisions. *Methods*: In this study, pedestrian's age, collision angle and pedestrian's position are considered influencing factors. Nine experiments using a novel lower extremity mechanical model are designed with the orthogonal experiment method. *Results*: Under the same collision angle, collisions in the left and right positions caused more serious tibia injuries than the middle position. As for the collision angle, the tibial injury at +45° is more significant than the tibial injury at −45°, and the injury of oblique collisions is slightly greater than that at 0°. Moreover, tibial injury is more sensitive to research variables than femoral injury. When the collision angle and position are changed, the difference ratio of tibia stress is by 483.2% higher than that of femur stress. The axial force and bending moment of the quadriceps tendon in the left-position collision reach peak values, which are 3.83 kN and 165.98 Nm, respectively. The peak quadriceps tendon axial force is captured with the collision angle of −45°, and the peak quadriceps tendon bending moment is obtained with a collision angle of +45°. *Conclusions*: The effects of differences in impact position and angle on lower extremity injury in the elderly were analyzed, and the results of this study can be used as a reference for research on lower extremity protection.

Key words: *lower extremity injury, car–pedestrian collision, impact position, impact angle*

1. Introduction

The safety protection of elderly pedestrians has been the focus of passive safety research on collision accidents. Developments in the automotive industry have provided convenience for people, but traffic accidents also threaten road users. In traffic accidents, pedestrians are road users with a high casualty and injury rates because of insufficient protective measures. In addition, the risk of lower extremity injury is exceptionally high in car–pedestrian accidents, accounting for 32.8% of the total crash injury [17]. The injury rate of the lower limbs is significantly high, which is the leading cause of disability [14]. The lower extremities of road users, especially pedestrians, are not well protected. Therefore, reducing the risk of the lower extremity injuries of pedestrians in accidents by investigating the characteristics of lower extremity injuries is of great importance.

Different impact conditions inevitably lead to the different injury outcomes of pedestrians' lower extremities. Valuable insights into the injury characteristics of pedestrians' lower extremities can be obtained by analyzing and understanding different collision factors. Wang [22] analyzed pedestrian accident cases in the German In-Depth Accident System, including the impact of collision speed, pedestrian age, height and weight on the risk of serious injury to pedestrians' lower extremities. He then studied the relationship between different collision factors and pedestrian lower limb AIS2+ and injury risk through logistic regression analysis. Klinich [10] analyzed statistical data and concluded that pedestrian age is significantly associated

* Corresponding author: Xiaoang Liu, School of Mechanical Engineering, Hebei University of Technology, Tianjin 300401, China. E-mail: liuxiaoang@hebut.edu.cn
Received: December 23rd, 2022
Accepted for publication: March 31st, 2023

with AIS2+ injury and lower extremity fracture risk. Klein's research on the effect of age differences on lower extremity injuries showed that lower extremity skeletal tolerance gradually decreases with age. Under the same impact loading, elderly people are more likely to be seriously injured in a crash [9]. In summary, age is an important factor affecting lower extremity injuries. However, pedestrians are not the only elements in traffic accidents, and collision conditions considerably influence injury. Thus, a study considering age and complex collision conditions is urgently needed.

In most vehicle–pedestrian collisions, the front--ends of vehicles directly hit a pedestrians' lower limbs. Therefore, the structure and characteristics of a vehicle's front-end can significantly influence pedestrian injury. The injury mechanism of occupants and pedestrians was different. The injury of occupants mainly depend on the restraint system, while the injury of pedestrians depend on the vehicle shape and stiffness [8], [23]. By performing 20 experiments, Bunketorp [2] compared the effects of the different front-end structures of vehicles on pedestrian injuries. He pointed out that optimizing the height of the front-end structure can reduce the level of pedestrian lower extremity injury. Mo [13] established 98 sets of finite element simulation models to study the impact of various vehicle front-end designs on pedestrian knee ligament and tibia injuries. Huang [4] conducted collision simulations with a vehicle model and a lower extremity impactor, and the results indicated that the curvature of the front-end structure affects lower extremity injury. The above studies have shown that the structure and stiffness of the front-end of a vehicle greatly influence the lower extremity injuries of pedestrians. However, actual accident conditions are diverse, and pedestrians might collide with the front of the vehicle at different positions and angles. Therefore, lower extremities injuries caused by the front-end of the car in different collision angles and collision positions should be further explored.

Traffic accidents might occur at any collision directions because of complex urban road conditions. Some studies have verified pedestrian lower limb injuries at different collision angles. Liu [11] analyzed the influence of different collision angles on the injury of the lower extremity mechanism and concluded that the injury risk of side collision is higher than that of a frontal collision. Ashton [1] pointed out that in side collisions, the lower limbs suffer multiple injuries because of the action of lateral force and axial load. Kajzer studied the effect of load on pedestrian lower limbs injury by performing a lower limb impact test [6], [7]. These studies mainly investigated influence on lower extremity injuries under frontal and side impact conditions. However, contact between pedestrians and vehicles in real-world traffic accidents occur at different angles, and pedestrian injury in oblique collisions still needs further research.

Different lower extremity injury criteria have been used to assess lower extremity injuries in pedestrians. Tolea [21] analyzed the impact forces acting on the lower extremity and estimated the severity of the injury based on the bending moment of the tibia. Tian [20] studied the effect of determining the hip flexion angle on the trend of lower extremity injuries. Most of these studies selected fewer injury criteria for assessing lower extremity injuries and had less mechanical analysis of lower extremity injuries. Therefore, there is a need to explore the mechanisms of lower extremity injury using various injury criteria combined with mechanical analysis.

Elderly pedestrian safety is a growing concern in traffic crashes. Investigating elderly pedestrian lower extremity injuries in collisions is essential. The purpose of this study is to conduct vehicle–pedestrian collision simulations at different oblique angles and collision positions to analyze the characteristics of lower extremity injuries.

2. Materials and methods

2.1. Lower limb model of the elderly

Human characteristics and geometric differences varied from country to country. Therefore, the previous human lower extremity model developed cannot represent the Chinese human lower extremity model [25]. To accurately predict injuries in Chinese pedestrians, a Chinese pedestrian human active lower extremity model was used in this study (Fig. 1), and some of the modeling details of this model have been reported previously [15], [16]. Given the influence of age, the lower extremity model was selected for the elderly with a greater risk of injury. In the establishment of the lower extremity model, age difference was mainly distinguished by the material parameters of bones in the lower extremity. The mechanical properties and characteristics of the elderly change with calcium loss because of age, and their bones become loose because their mechanical properties change. This change was highlighted according to differences in bone material parameters (Table 1), and these parameters were with reference to the experiment [12].

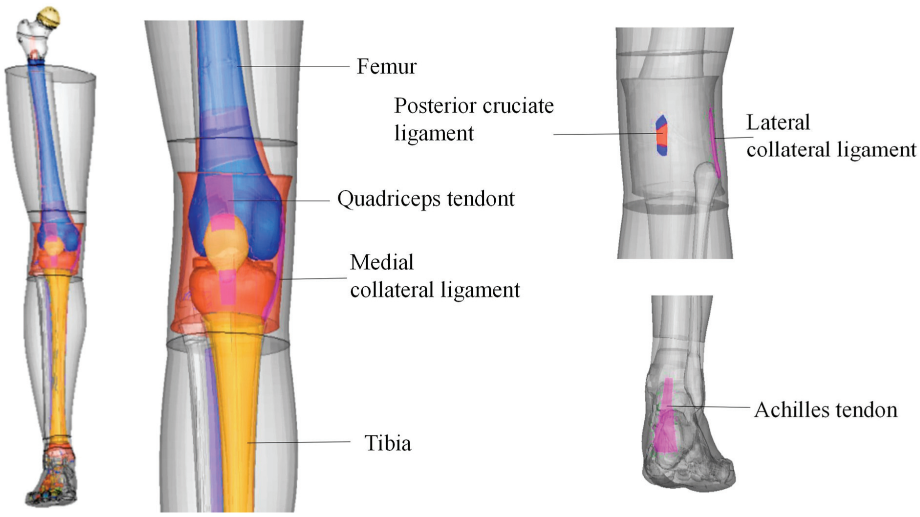

Fig. 1. Lower extremity model of the elderly

Finite Element (FE) simulation is an efficient method for implementing multiple groups of collision simulations. Moreover, the lower limb FE model contains 106,827 elements and 97,010 nodes. To simulate the influence of the upper body weight, a uniform loading of 400 N was applied to the femoral head joint. Internal contact between components was mainly the automatic single-surface contact between tissues. This model has been conducted to have high biofidelity through the shear test and the displacement time curve obtained from the elder cadaver experiment [11]. At last, the LS-Dyna solver was used to implement the FE calculation process.

Table 1. Material parameters in the lower limb of the elderly

	Femoral shaft	Tibial shaft
Density [kg/mm^3]	2×10^{-6}	2×10^{-6}
Elastic Modulus [GPa]	13.290	15.020
Poisson's ratio [–]	0.3	0.3
Yield stress [MPa]	75	88.94
Tangent modulus [GPa]	1.0	1.4
Plastic failure strain [–]	0.0140	0.0129
Strain rate parameter C [–]	360.5	360.5
Strain rate parameter P [–]	3.605	3.605

2.2. Analytical model of lower limb impact

The stress distribution in the lower extremity is an important indicator for evaluating lower extremity injuries. Usually, cracks or even fractures may occur in the areas of stress concentration, and more attention should be paid to evaluating injuries [24]. The collision mechanics analysis can reflect the stress magnitude of the lower extremity in detail, which helps to better understand the collision mechanism. Based on the curved beam model established by Jiang [5], the femur was simplified to a segment of curved beam with an initial curvature of approximately sinusoidal form (Fig. 2), and the femur was assumed to have a uniform cross-section and consist of isotropic material.

Suppose the length of the curved beam is L and the initial maximum deflection is a. The initial coordinates of each point of the curved beam are as follows:

$$y_0 = a \sin\left(\frac{\pi x}{L}\right); \quad x_0 = x. \tag{1}$$

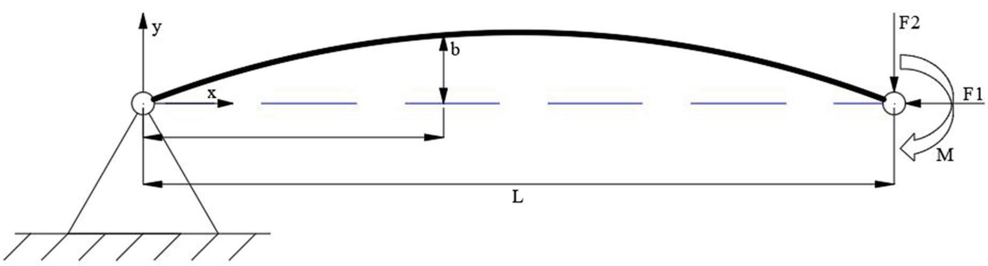

Fig. 2. Schematic diagram of the forces on the femur

When subjected to a combined pressure-bending load, the deflection at any point b on the curved beam increases by y, then, the bending moment at that point can be deduced from:

$$M_b = \frac{Mx}{L} + F_1(y + y_0) + F_2(L - x_0)\,. \qquad (2)$$

According to the differential equation of the deflection curve:

$$EI\frac{d^2y}{dx^2} = -M_b = -F_1(y + y_0) - F_2(L - x_0) - \frac{Mx}{L}\,, \qquad (3)$$

where: F_1 is the axial pressure, F_2 is the radial pressure, M is the bending moment load at the thigh end of the femur, E is the modulus of elasticity, and I is the radial moment of inertia.

Substituting Eq. (1) into Eq. (3) yields:

$$\frac{d^2y}{dx^2} + \frac{Mx}{EIL} + \frac{F_1\left(a\sin\left(\frac{\pi x}{L}\right) + y\right) + F_2(L - x)}{EI} = 0\,. \qquad (4)$$

Solving the binary differential equation:

$$y = C_1\cos\left(\sqrt{\frac{F_1}{EI}}x\right) + C_2\sin\left(\sqrt{\frac{F_1}{EI}}x\right) + \frac{aF_1L^2}{\pi^2EI - F_1L^2}\sin\left(\frac{\pi x}{L}\right) + \frac{(F_2L - M)}{F_1L} + \frac{F_2L}{F_1}. \qquad (5)$$

According to the initial condition $x = 0$ or L when $y = 0$, substituting this condition into Eq. (5) gives:

$$C_1 = -\frac{F_2L}{F_1};\quad C_2 = \frac{F_2L\left[\cos\left(\sqrt{\frac{F_1}{EI}}L\right) - 2\right] + M}{F_1\sin\left(\sqrt{\frac{F_1}{EI}}L\right)}. \qquad (6)$$

Substituting Eq. (1), Eq. (5) and Eq. (6) into Eq. (2) yields the bending moment at point b as:

$$M_b = -F_2L\cos\left(\sqrt{\frac{F_1}{EI}}L\right) + \frac{F_2L\left[\cos\left(\sqrt{\frac{F_1}{EI}}L\right) - 2\right] + M}{\sin\left(\sqrt{\frac{F_1}{EI}}L\right)} \sin\left(\sqrt{\frac{F_1}{EI}}x\right) + \frac{\pi^2aEIF_1}{\pi^2EI - F_1L^2}\sin\left(\frac{\pi x}{L}\right). \qquad (7)$$

In a section subjected to a bending moment, the stress on the part of the section at a distance c from the neutral plane where no deformation occurs:

$$\sigma = \frac{M_bc}{I}\,. \qquad (8)$$

When point c is at the uppermost and lowermost edges of the section, it corresponds to the maximum tensile and compressive stresses, respectively. When the tensile and compressive stresses reach the material failure value, the femur fracture occurs at the corresponding area.

This stress equation enables preliminary stresses to be obtained at any point on the femur. Analysis of the risk of injury to the lower extremity shows that when the radial pressure at the end of the femur increases, the stress on the pedestrian's leg subsequently increases. In addition, the bending moment at the end of the femur also affects the stresses applied to the femur, and different collision angles affect the bending moment at the end of the femur, indicating the need to consider the effect of different collision angles on the pedestrian lower extremity during a car–pedestrian collision.

2.3. Injury criteria

Bone fractures and knee injuries are the most common symptoms of pedestrian lower extremity injuries [8]. Stress in the femur and tibia, bone fractures, ligament tension, and ligament distortion are essential factors for evaluating lower extremity injuries. Therefore, in the comprehensive analysis of the characteristic of lower extremity injury, the stress distribution of the femur and tibia, the axial force of the knee ligaments and the bending moment of the knee ligaments were selected as characterization quantities. Medial collateral ligament (MCL), lateral collateral ligament (LCL) and posterior cruciate ligament (PCL) were used as target ligaments for measurement. Given the tendon injury, the Achilles tendon (AT) and quadriceps tendon (QT), were selected for the evaluation of lower extremity injuries (Fig. 1).

2.4. Simulation matrix

Collision position and collision angle are unpredictable in car–pedestrian accidents, and injury outcomes under different collisions are bound to be different. Therefore, studying lower limb injury characteristics with different collision positions and angles is essential. Given that car–pedestrian accidents are common in urban roads, a relatively low collision velocity of 25 km/h was applied to the experiment. Toyota Camry is a sedan with a high market share, and its front structure is representative. Therefore, the Camry FE model was used in this study for the 25 km/h collisions.

In this study, the orthogonal experiment method was used, and three levels of collision positions and collision angles were used in pedestrian–vehicle collision simulations (Table 2).

Table 2. Simulation matrix

	Impact direction		
Relative position	+45°	−45°	0°
Left side of the car	T1	T2	T3
Right side of the car	T4	T5	T6
Mid of the car	T7	T8	T9

The collision position referred to the position where the front-end of the vehicle directly contacted the pedestrian, and the collision angle referred to the angle between a vehicle and pedestrian. As for the selection of research variables, three collision positions were designed. Left, middle and right positions were used. Because of the uncertainty of the collision angle in human–vehicle collisions [18], the collision angles in three directions were selected. The frontal collision between the lower limb and the vehicle (0°), the oblique collision with a collision angle of +45°, and the oblique collision with a collision angle of −45°. For the above collision condition, nine groups with two variables with three levels (three collision positions and three collision angles) were designed in analyzing the collision process (Fig. 3).

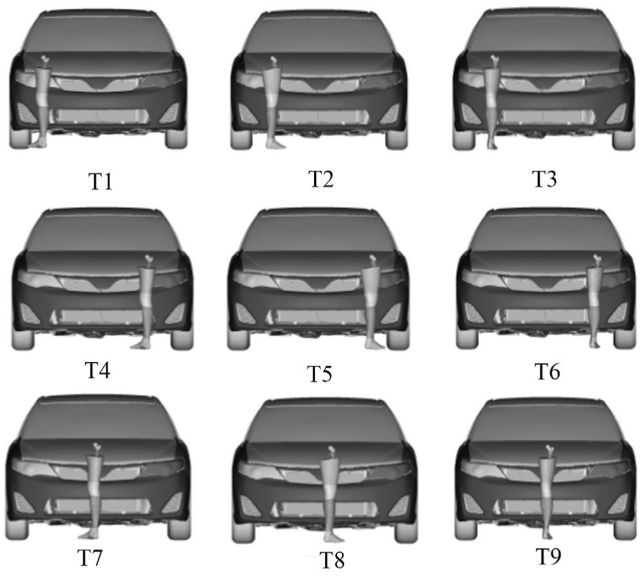

Fig. 3. Crashes under impact conditions

3. Results

3.1. Stress distribution of femur and tibia

To analyze the characteristics of the injury mechanism of the lower limbs, the stress distributions in the femur and the tibia were compared, and the injury characteristics under different collision conditions were obtained. The injury trend was analyzed by the peak value of the stress (Table 3) and changing trend.

Table 3. Peak stress in bones among simulations [MPa]

	Femur	Tibia
T1	93.10	51.37
T2	93.05	46.96
T3	92.75	42.36
T4	93.32	50.92
T5	92.01	41.38
T6	93.03	41.43
T7	90.46	46.72
T8	97.15	59.01
T9	92.14	39.36

The results showed that under all collision conditions, no obvious lower extremity fracture along the diaphysis was noted, and the peak stress of the femur was greater than that of the tibia (Figs. 4, 5). The maximum stress of the femur in all conditions was 97.15 MPa, which was observed at T8. The minimum stress was 90.46 MPa and was observed at T7. The difference between the maximum peak stress and minimum peak stress of the femur was 6.69 MPa, and the stress difference ratio was 6.89%; however, except for T8, the difference of the femoral injury in the other conditions was insignificant. The maximum stress of the tibia was 59.01 MPa, which was obtained in T8, and the minimum stress peak was 39.36 MPa, which was obtained in T9. The highest risk of injury in T8 was inseparable from the physiological structure of the lower limbs. When the right lower limb of the human body was deflected to the right and bent at the same angle, it required more energy than the left side. In T8, the lower limbs were in the middle position, and the lower limb tended to deflect to the right, and thus the stress value in T8 was the highest. The difference between the maximum peak stress and the minimum peak stress of the tibia was 19.65 MPa, and the stress difference ratio was 33.29%. The peak tibia stress levels of T1, T4, and T8 were over 50 MPa, and the peak tibia stress levels of T3, T5, T6, and T9 were all around 40 MPa. In all experiments, the stress concentration areas of the femur were small, whereas the stress concentration areas of the tibia were relatively large. The stress concentration areas of the femur were located on the upper end of the femur, whereas the stress concentration areas of the tibia were located on the upper and middle parts of the tibia.

Comparing the femoral and tibial stress distributions of T3, T6, and T9, femoral injury in the simulation was concentrated in the upper part rather than near the center of gravity because the mass of the upper body was much greater than that of the foot during collision and the force on the hip was much greater than the force on the foot and the force near the center of gravity of the femur. The stress concentration area of the femur was located at the upper end of the femur. However, given that the forces in the foot were not significant, the stress concentration area of the tibia was mainly located at the center of gravity of the tibia.

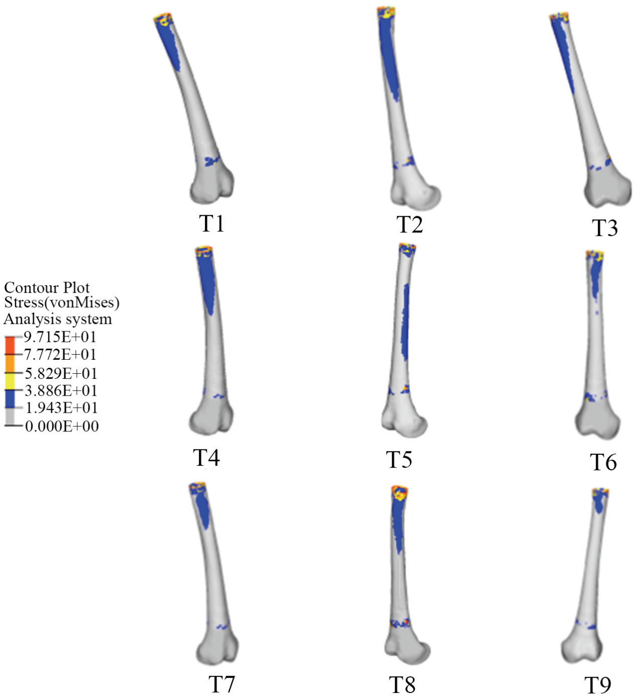

Fig. 4. Femur stress distribution

The analysis the above results shows that the possibility of lower extremity fractures when pedestrians and vehicles collide at low speeds was relatively low. Under all collision conditions, the maximum femur stress was 97.15 MPa and the maximum tibia stress was 59.01 MPa. Difference in the ratio of femoral injury was 6.69% between different experiments, and the difference in injury risk was minimal. This result indicated that the femoral injury was not sensitive to the collision angle and collision position. By contrast, the difference ratio of tibial injury was 33.29% and the risk of injury varied greatly. Tibial injury was more sensitive to two collision factors. As for the collision angles, under the +45° oblique collision and 0° collision, difference in tibial injury in the left and right collision positions was greater than that in the middle collision position. However, under the −45° oblique collision condition, the injury risks of the three collision positions were quite different. The tibia injury of the middle collision was larger than that of the left and right collision.

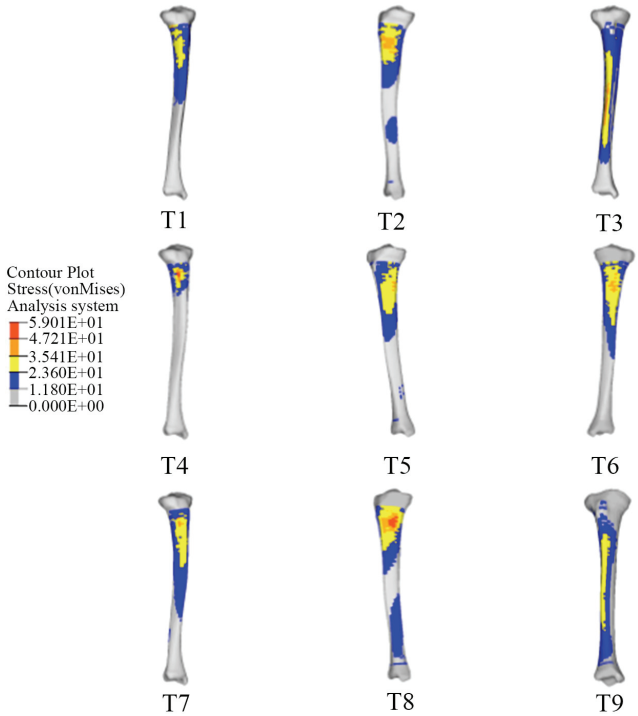

Fig. 5. Tibial stress distribution

In the three collision conditions of T1, T4, and T8, the peak tibial stress was above 50 MPa, and the peak tibial stress was about 40 MPa in T3, T5, T6, and T9. Tibia injury risk under +45° and −45° collision was greater than that in a 0° collision. In the three groups of experiments with the same collision position but different collision angles, tibial injury risk was greater than that of the −45° collision in the left and right positions. The risk of tibial injury in the +45° collision was slightly greater than that in the 0° collision. In the middle position, the −45° collision had greater tibia injury risk than the +45° and 0° collisions. The reason for this difference might be that lower limbs tended to slide to the outer edge during the left and right side collisions, resulting in high stress in the +45° oblique collision condition. By contrast, the lower extremity directly collided with the front of the car in the middle position collision. The reason for sliding to the side and causing −45° may be that the lower limbs tend to slide to the outer edge when the left and right sides collide. This sliding may cause the most severe injury during +45° collision.

The results of the study on the influence of different collision positions and collision angles on lower limb injury characteristics showed that the left and right collision positions cause more serious injuries than the middle collision position. The injury risk of the +45° collision was greater than that of the 0° collision. Right and left collisions with a +45° angle had the greatest risk of injury, and the injury risk of the middle position collision was the highest when the collision angle was −45°.

3.2. Axial force and bending moment

Axial force and the bending moment of the lower extremity were commonly used as evaluation indices in lower extremity biomechanical tests. In this study, the mechanical characteristics of lower extremity injury with different collision positions and collision angles were obtained. After the analysis of experimental data, the force and bending moment values of the measured locations, except for AT, became stable at 30 ms after the collision. Thus, the collision time was set at 40 ms after the collision, except for the AT, whereas the collision time of AT was set at 80 ms (Figs. 6, 7). Under all conditions, the maximum of peak force and peak bending moment of the QT were 3.83 kN and 165.98 Nm, respectively. The maximum peak force and peak bending moment of the MCL were 0.54 kN and 1.59 Nm, respectively. The maximum peak force and peak bending moment of LCL were 0.42 kN and 0.68 Nm, respectively, and the maximum of peak force and peak bending moment of AT were 0.38 kN and 1.05 Nm, respectively. The maximum of peak force and peak bending moment of the PCL were 3.39 kN and 23.57 Nm, respectively.

Comparing the peak force and bending moment at five measurement locations, the peak force of the QT was 2.54–3.83 kN, and its bending moment was 80.92–165.98 Nm. The peak force of PCL was 2.65–3.39 kN, and its bending moment was 13.69–23.57 Nm. By contrast, the maximum peak force of the other three measurement locations did not exceed 0.55 kN, and their maximum bending moment did not exceed 1.59 Nm. The QT and PCL were the most injured locations. The force of the QT was close to that of the PCL, but the bending moment of the QT was

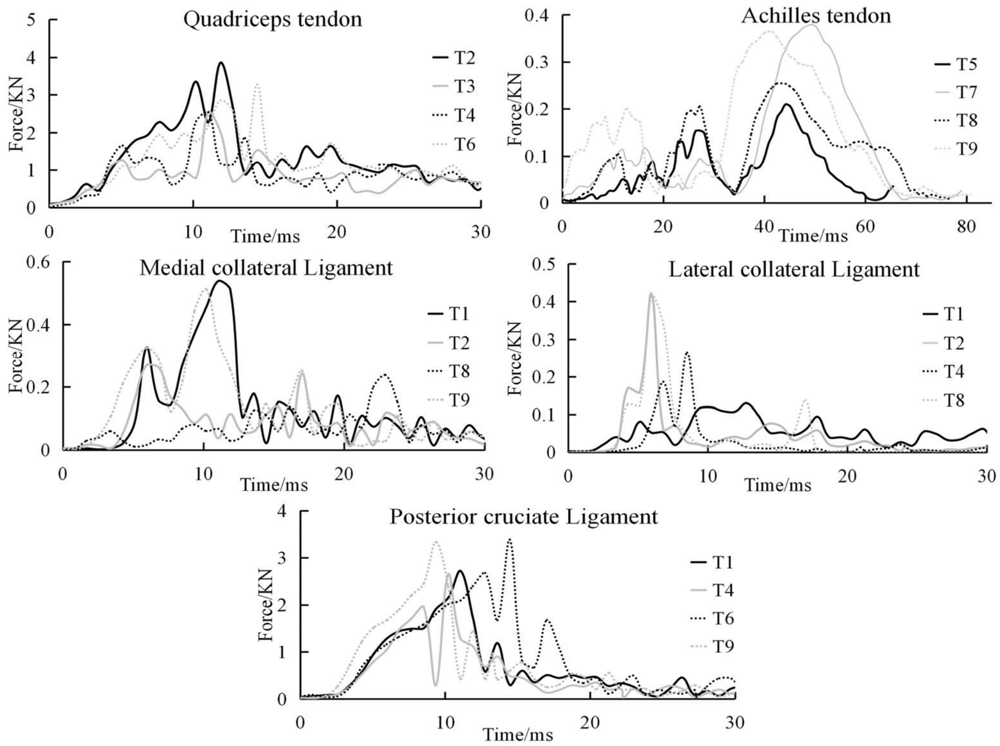

Fig. 6. Ligament force at the measurement location

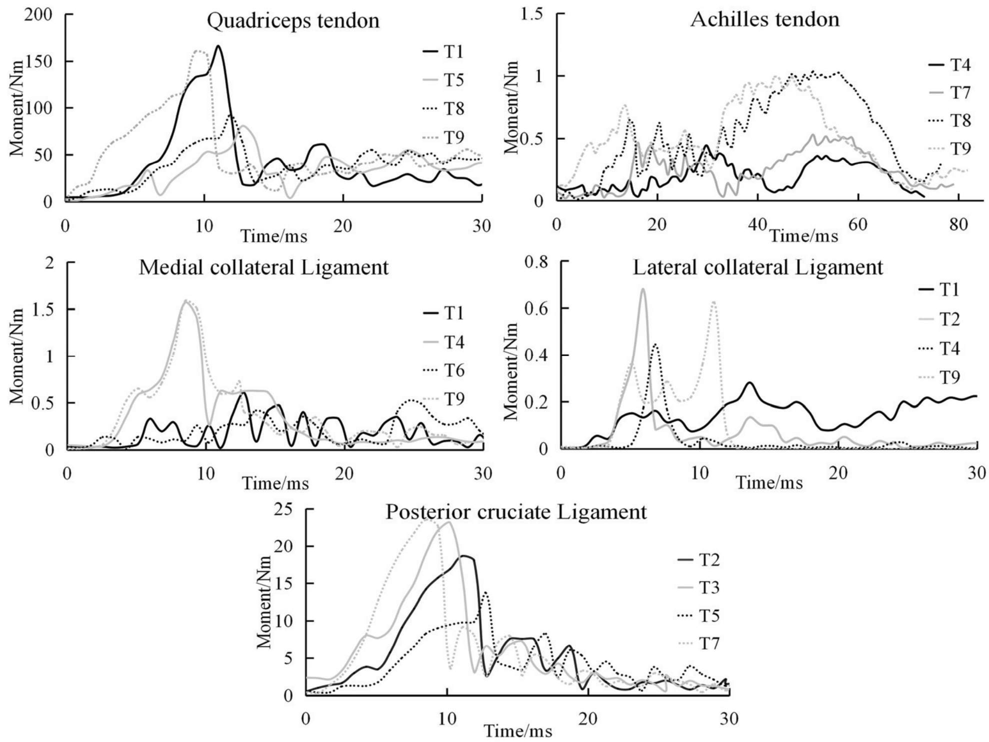

Fig. 7. Bending moment at the measurement location

much greater than that of the PCL. Thus, the QT was the most vulnerable location of the measured position of the lower limb. The force and bending moment of the QT, MCL, LCL, and PCL all reached their peak values within 10 ms after collision. The AT reached its peak values within 40–50 ms after collision. This result might be related to differences among the positions of the measured ligaments. The four measurement positions, including the QT, were all located at the knee. The knee of the pedestrian was directly impacted when collision occurred, whereas AT did not collide. Therefore, the peak force and bending moment of the AT was observed later than the other four measurement positions.

The maximum peak force of the QT was 3.83 kN and occurred in T2, whereas the minimum peak force of QT was 2.54 kN and occurred in T4. Difference between these peak forces was 1.29 kN. The maximum peak stress of the PCL was 3.39 kN and occurred in T6, which was slightly larger than that of T9 with a peak stress of 3.38 kN. The minimum peak stress of PCL was 2.65 kN and occurred in T4, which was slightly smaller than that of T1 with a peak stress of 2.72 kN. The difference between the maximum and minimum peak stress of PCL was 0.74 kN. At a collision angle of +45°, the force of the QT and PCL was less than that of the −45° and 0° collision. The peak stress of the QT was the highest under the −45° collsion. The peak stress of PCL was the highest at a 0° collision. The maximum peak bending moment of the QT was 165.98 Nm, which was observed in T1. The minimum peak bending moment of the QT was 80.92 Nm, which was observed in T5. The difference between the maximum and minimum peak bending moment of the QT was 85.06 Nm. The maximum bending moment of the PCL was 23.57 Nm, which was observed in T7, and the minimum bending moment of the PCL was 13.69 Nm, which was observed in T5. The difference in bending moment between T7 and T5 was 9.88 Nm. The largest peak bending moment of the QT and PCL was obtained during +45° collision. However, the smallest peak bending moment of the QT and PCL was obtained during the −45° collision. Summarizing, collision angle had a stronger influence on lower extremity injury than collision position according to the analysis of the nine impact conditions.

Given that the QT was the most vulnerable part among the measurement locations, a detailed analysis of the injury characteristics of the QT with the difference in collision angle and position was carried out.

QT injuries in the three experiment groups (T1, T4, T7; T2, T5, T8; T3, T6, T9) were observed at the same collision angle but different collision positions (Fig. 8). In the peak QT stress, when the angle between the pedestrian and vehicle was +45°, the peak stress of the left collision (T1) was the highest, whereas the peak stress of the right collision (T4) was the lowest. When the angle between the pedestrian and the vehicle was −45°, the peak stress of the left collision (T2) was the highest, whereas the peak stress of the right and middle collision (T8, T5) was the lowest. When the angle between the pedestrian and vehicle was 0°, the peak stress of the right collision (T6) was the highest, whereas the peak stress of the left collision (T3) was the lowest. As for the QT's peak bending moment, the results obtained from the three groups of experiments had the following sequences: T1 > T7 > T4, T2 > T8 > T5, and T9 > T3 > T6.

The maximum peak axial force in the three groups were 3.27 kN (T1), 3.83 kN (T2), and 3.28 kN (T6). Collision in T1 and T2 occurred in the left side, and the collision position of T6 was the right side. The minimum peak axial force was 2.54 kN (T4), 3.15 kN (T5), and 2.55 kN (T3). Among the three groups, the maximum bending moment was 165.98 Nm in T1, 121.79 Nm in T2, and 160.36 Nm in T9. Moreover, collision in T1 and T2 occurred at the left position, and collision in T9 occurred at the middle position. The minimum bending moment was 134.31 Nm in T4, 80.92 Nm in T5, and 115.43 Nm in T6, and collision under three impact conditions occurred on the right side. Analyzing of the above results, it can be stated that the axial force and bending moment of the QT at the left collision position were greater than that at the middle or right position.

Three groups (T1, T2, T3; T4, T5, T6; T7, T8, T9) of QT injuries with the same collision position and different collision angles were obtained (Fig. 9). In the experiment groups with the left collision position, the peak force had the following order: T2 > T1 > T3, and the peak bending moment had the following order: T1 > T3 > T2. As for the right collision position, the peak force had the following order: T6 > T5 > T4, and the peak bending moment had the following order: T4 > T6 > T5. In the middle collision position, the peak force had the following order: T8 > T9 > T7, and the

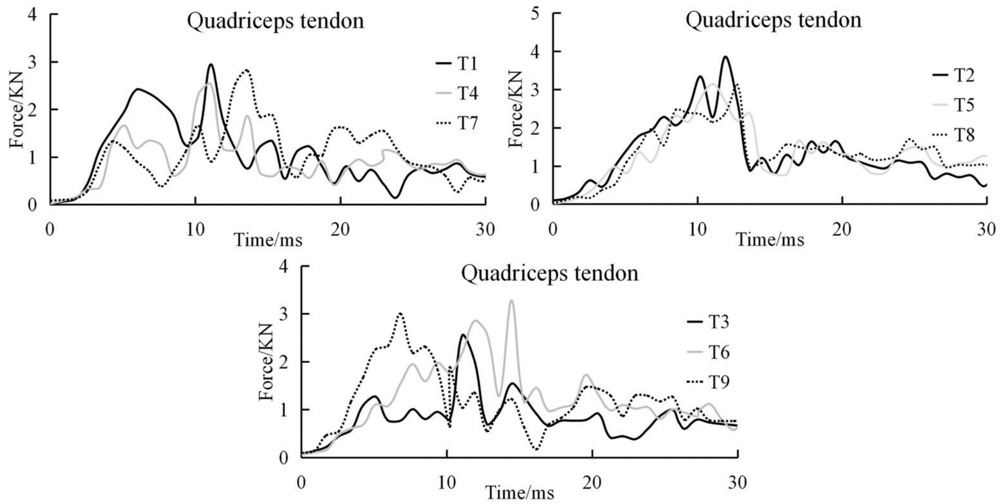

(a) ligament force

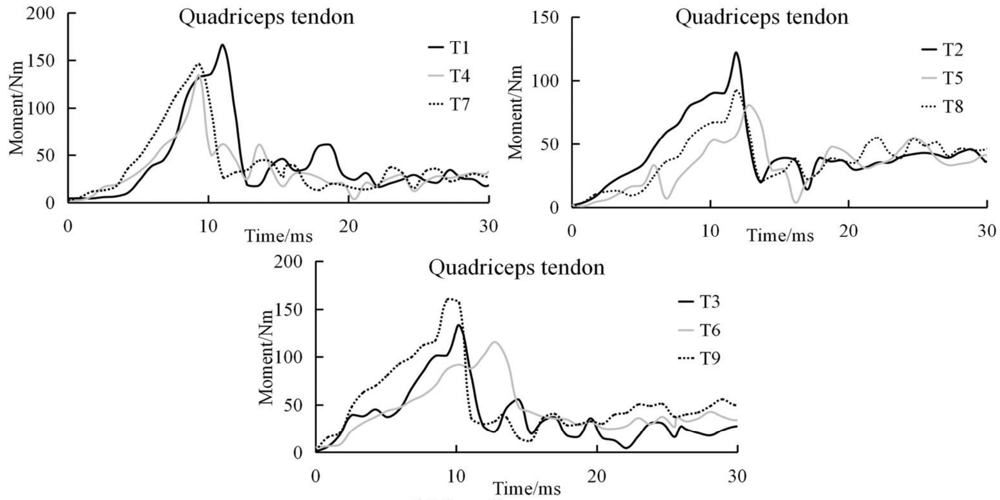

(b) bending moment

Fig. 8. QT force (a) and bending moment (b) with different collision positions

peak bending moment had the following order: T9 > T7 > T8.

The maximum peak stress was 3.83 kN in T2, 3.28 kN in T6, and 3.13 kN in T8. Moreover, the collision angles of T2 and T8 were −45°, and the collision angle of T6 was 0°. The minimum peak force was 2.55 kN in T3, 2.54 kN in T4 and 2.81 kN in T7. The maximum peak force of T6 was 3.28 kN when colliding at the right position possibly because of the physiological structures of the lower limbs. After a collision on the right side, the lower limbs tended to slide to the right. However, the maximum peak force of T6 and T5 was approximate, the peak force of T5 was 3.15 kN, and the collision angle of T5 was −45°. Therefore, from the perspective of bearing axial force, the injury risk of QT injury was the greatest at the −45° collision angle when the collision position was the same. As for the bending moment, the maximum bending moment was 165.98 Nm in T1, 134.31 Nm in T4, and 160.36 Nm in T9. The minimum bending moment was 121.79 Nm in T2, 80.92 Nm in T5, and 92.53 Nm in T8. The maximum bending moment of T9 was 160.36 Nm when colliding in the middle position because T9 collided in the middle position and the collision angle was 0°. In this case, the lower limb would bend directly forward, and the QT suffered the greatest bending moment. However, the maximum peak bending moments of T7 and T9 were approximate. The peak bending moment of T7 was 146.22 Nm, and its collision angle was +45°. Therefore, from the perspective of bending moment, the risk of QT injury was the greatest under the +45° condition when the collision position was the same.

When the collision position was the same, the QT had the highest force and lowest bending moment at the −45° collision angle. Meanwhile, the QT had the lowest force and highest bending moment at the +45° condition collision angle.

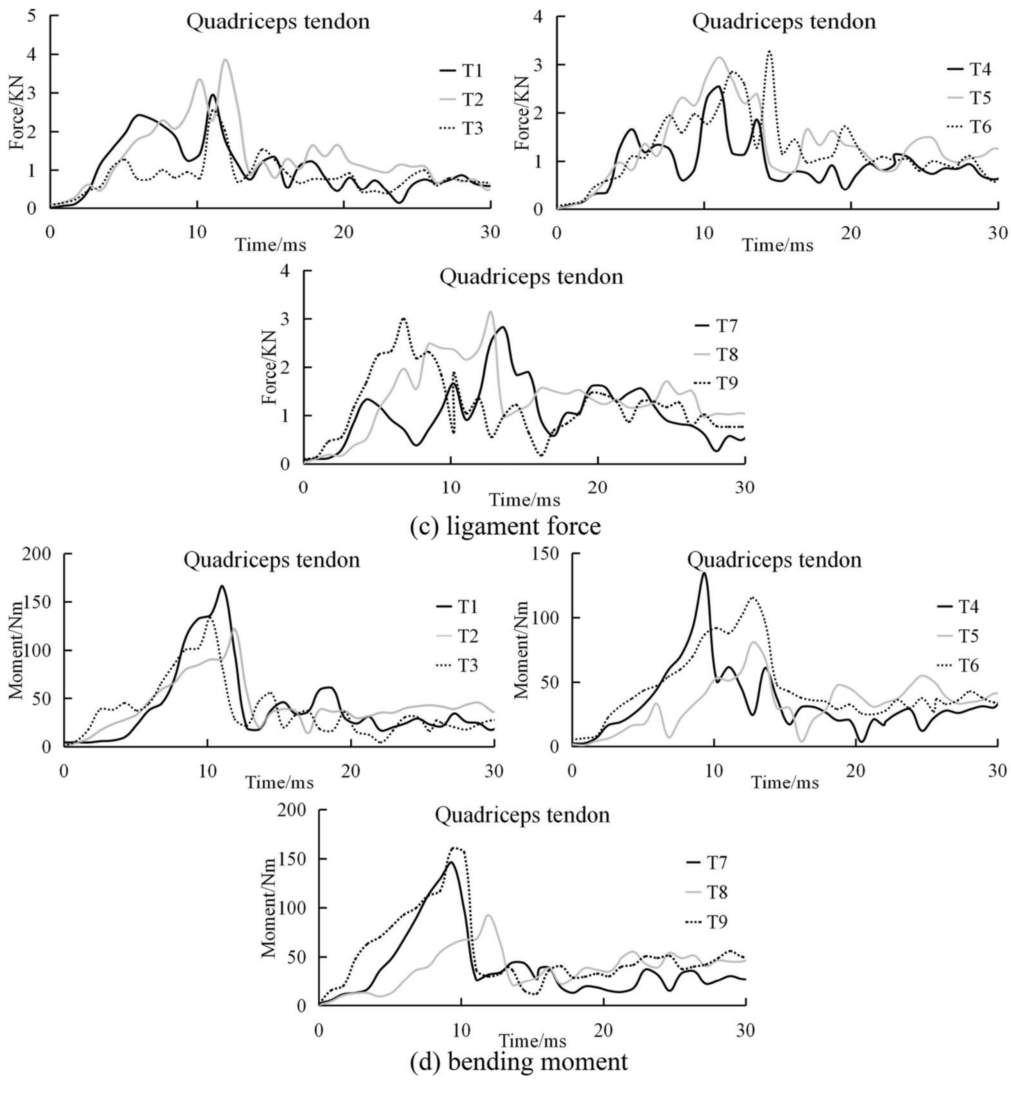

Fig. 9. QT force (c) and bending moment (d) with different collision angles

4. Discussion

4.1. Injury trend of femur and tibia

Owing to the complexity of traffic roads, predicting the relative position and relative angle of vehicle–pedestrian collision when an accident occurs is difficult. In a car collision, different collision positions are accompanied by differences in the radian and stiffness of the front-end structure of the car, which in turn affects the characteristics of lower extremity injuries. At different collision angles, the front end of a car collides with the different positions of the pedestrian's lower limbs, and difference in collision position affects the motion and force characteristics of the lower limbs. The coupling analysis of the car–pedestrian collision at the different collision angles and collision positions shows that the risk of femoral injury is greater than the risk of tibial injury under the nine conditions. By analyzing the coupling of cars and pedestrians at different collision angles and collision positions, as well as their multivariate and interaction plots of femoral and tibial stress distributions, the results shows that the risk of femoral injury is greater than the risk of tibial injury under the nine conditions (Fig. 10). However, in all experiments, the difference ratio of femur injury is 6.89%. Notably, difference in femur injury is slight, and the femur injury is not sensitive to the two impact factors. By contrast, difference in the ratio of tibial injury is higher than that of the femur, with a value of 33.29%. This result suggests that tibial injury has a more significant change when the impact angle and position change and tibial injury is more sensitive to these collision factors.

From the perspective of collision position, the left and right collision positions pose a more moderate threat to the tibia than to the middle collision position. Specifically, the average tibia force of the left collision is 46.89 MPa, and the average tibia force of the right collision is 44.58 MPa. The average tibia force of the middle collision is 48.36 MPa. These tibia forces are inseparable from the structure of the front end of the car. The radian of the structure at the left and right ends of the car is greater than the radian of the middle position of the car. When a car collides on the left or right sides, the tibia tends to move laterally to both ends, and this movement affects the interaction force between the tibia and various joints and difference in tibia injury at different positions. From the perspective of collision angle, when the collision angle is +45°, the average femur force is 92.29 MPa, and its average tibia force is 49.67 MPa. When the collision angle is −45°, the average femur force is 94.07 MPa, and its average tibia force is 49.12 MPa. When the collision angle is 0°, the average femur force is 92.64 MPa, and its average tibia force is 41.05 MPa. From the overall results, there is an interaction between the two impact factors. In summary, the lower extremity injury risk caused by oblique collision is higher than that of the 0° collision. Moreover, the highest injury risk at +45° angle is observed in the right-side collision, and highest injury risk at −45° angle is observed in the middle collision. This result is mainly caused by the physiological structure of the elderly's lower extremity, and

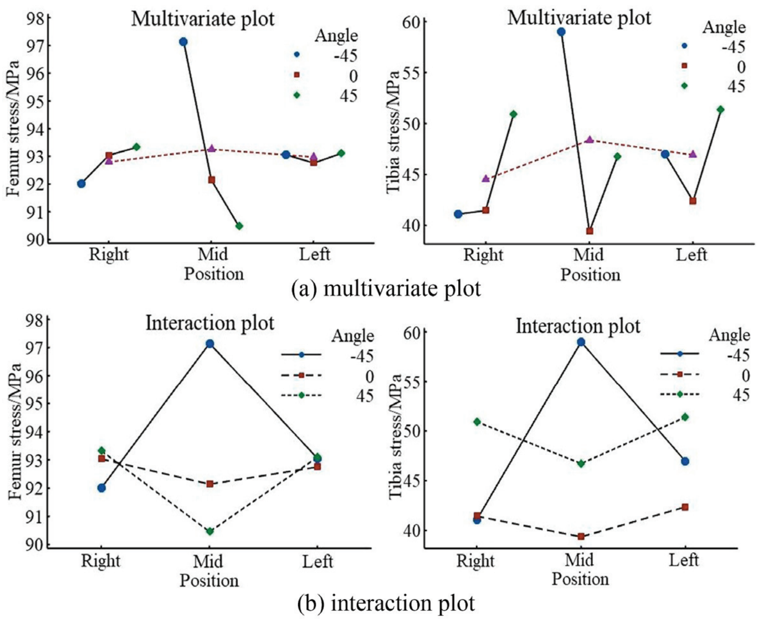

Fig. 10. Multivariate plots (a) and interaction plots (b) of femoral and tibial stress distribution

the interactions among the different parts of the lower extremity are inevitably be affected after the collision of different parts, thereby affecting the tibia injury of the lower extremity. These results are similar to those of Chen [3], who stated that injury to the lower limb is greater in lateral collisions and injuries caused by different vehicle materials vary. However, the differences in lower extremity physiological structure under different collision positions and the differences in lower extremity movement trends under different oblique collisions may have influence on characteristics of lower extremity injuries.

4.2. Trend of ligament injury

Knee injuries account for a large proportion of lower extremity injuries in previous research. Especially in the elderly, knees are more prone to injury. This research studies the mechanism and characteristics of knee ligament, QT and AT injuries, which have been comprehensively studied through the comparative analysis of nine impact conditions. By comparing and analyzing the axial force and bending moment of five injury measurement locations, it was found that the QT and the PCL are the positions with higher number of injuries. By contrast, the LCL, MCL, and AT are not vulnerable. Moreover, the most vulnerable part of the measurement locations is the QT. Huang [4] conducted a collision simulation experiment with a vehicle and a lower limb impactor, and the results showed that the difference in the curvature of the front end of the vehicle would affect knee joint injury. Research by Teresinski [19] on pedestrian injury accidents found that significant differences among knee joint injuries caused by impacting pedestrians from four positions: front, rear, left, and right. In this study, the difference between QT force and the bending moment is more than 50% when the collision position changes. This shows that knee injuries are extremely sensitive to changes in collision position, supporting the viewpoint of Teresinski.

In this study, injuries in the knee ligaments and tendons were investigated, and the mechanical characteristics of lower extremity injury at different collision positions and different collision angles were compared and analyzed. The influence of the collision angle factor is more significant than that of the collision position factor. In the tilt angle collision, there is always the axial force and bending moment of QT under the left collision position are greater than the middle or right side. At the same collision position, the QT ligament force at –45° is greater than the QT ligament force at 45°, while the QT bending moment at –45° is smaller than the QT bending moment at 45°, while the results at 0° collision are not significant. These differences in injury characteristics result from differences in the physiology of the lower extremity. Under different collision angles, the motion of the QT is influenced by the tendency of joint motion, which in turn leads to differences in lower extremity QT injury at different collision angles.

4.3. Coupling analysis of differences in collision factors

Based on the comparison of the orthogonal coupling experiments, it can be stated that both collision factors have an influence on the risk of lower extremity injury, but the influence of collision angle was more significant than the effect of collision position. In this study, femur injury is insensitive to changes in collision angle and position, whereas tibial injury is susceptible to the two factors. The influence of the different collision angles and different collision positions on the risk of tibial injury are analyzed, respectively. Tibial stress changes are more obvious when impact angles vary. The axial force and bending moment of knee ligaments and tendons under two kinds of impact factors were observed and analyzed. At different collision angles, changes in the axial force and bending moment are more significant than those at different collision positions. Therefore, under the research conditions of this paper, the collision angle factor has greater influence on lower extremity injury than impact position factor.

5. Conclusions

This research consisted of a detailed analysis and discussion on the injury of the lower limbs of the elderly from the macrolevel and microlevel perspectives, including the injury trend of any stress point of the leg bone, stress distribution, and changing trend of ligament force and bending moment. The study considers differences in age and impact load factor and analyzes the impact of differences in impact position and angle on lower extremity injuries in the elderly. This study found that both collision angle and collision position had an effect on lower extremity injury, and the effect of collision angle was more significant than that of collision position. Meanwhile, the risk of lower extremity injury was higher for tilt collisions than for 0° collisions at the same collision position. In addition, the QT was the most severely injured of all ligaments and tendons measured and the motion of the QT was influenced by the tendency of joint motion at different collision angles, which led to differences in QT injury in the lower extremity at different collision angles.

This study had two highlights. First, a new mechanical theoretical model of the femur was proposed. Second, based on a finite element model of the Chinese elderly, numerical analysis was used to reflect the trend of post-crash injury.

Acknowledgements

This study was supported by the National Natural Science Foundation of China (52175084), Natural Science Foundation of Hebei Province (E2020202017) and National Natural Science Foundation of China (52175085).

Conflicts of interest

The authors declare that they have no conflict of interest.

References

[1] ASHTON S.J., *Factors associated with pelvis and knee injuries in pedestrians struck by the fronts of cars*, SAE Tech. Pap., 1981, DOI: 10.4271/811026.

[2] BUNKETORP O., ROMANUS B., HANSSON T., ALDMAN B., THORNGREN L., EPPINGER R.H., *Experimental study of a compliant bumper system*, SAE Tech. Pap., 1983, DOI: 10.4271-831623.

[3] CHEN J.Q., CHENG R.J., LAN F.C., ZHOU Y.J., *Analysis of lower limb injury mechanism of an average Chinese pedestrian lower limb FE model in lateral impact*, Int. J. Veh. Saf., 2020, 11 (4), 330, DOI: 10.1504/IJVS.2020.111526.

[4] HUANG J.H., ZHENG W.Q., *Optimization design of vehicle front-end structure for pedestrian protection lower leg*, Mechanical Engineering and Automation, 2018, 6, 85–87.

[5] JIANG X., YANG J., WANG B., ZHANG W., *An investigation of biomechanical mechanisms of occupant femur injuries under compression-bending load*, Chinese Journal of Theoretical and Applied Mechanics, 2014, 46 (3), 465–474, DOI: 10.6052/0459-1879-13-282.

[6] KAJZER J., MATSUI Y., ISHIKAWA H., SCHROEDER G., BOSCH U., *Shearing and bending effects at the knee joint at low-speed lateral loading*, SAE Tech. Pap., 1999, DOI: 10.4271/1999-01-0712.

[7] KAJZER J., SCHROEDER G., ISHIKAWA H., MATSUI Y., BOSCH U., *Shearing and bending effects at the knee joint at high speed lateral loading*, SAE Tech. Pap., 1997, DOI: 10.4271/973326.

[8] KERRIGAN J., SUBIT D., UNTAROIU C., CRANDALL J.R., *Pedestrian lower extremity response and injury: a small sedan vs. A large sport utility vehicle*, SAE International Journal of Passenger Cars-Mechanical Systems, 2008, 1 (1), 985–1002, DOI: 10.4271/2008-01-1245.

[9] KLEIN K.F., HU J., REED M.P., SCHNEIDER L.W., RUPP J.D., *Validation of a parametric finite element human femur model*, Traffic Inj. Prev., 2017, 18 (4), 420–426, DOI: 10.1080/15389588.2016.1269172.

[10] KLINICH K.D., SCHNEIDER L.W., *Biomechanics of pedestrian injuries related to lower extremity injury related to lower extremity injury assessment tools: a review of the literature and analysis of pedestrian crash database*, 2003.

[11] LIU X.R., XIAO S., SUN X.X., *Research on lower extremity injury characteristics of elderly pedestrians under different impact loads*, Int. J. Crashworthines, 2022, 27 (5), 1287–1297, DOI: 10.1080/13588265.2021.1926846.

[12] MCCALDEN R.W., MCGEOUGH J.A., BARKER M.B., COURT-BROWN C.M., Age-related changes in the tensile properties of cortical bone. The relative importance of changes in porosity, mineralization, and microstructure, J. Bone Joint Surg. Am., 1993, 75 (8), 1193–1205, DOI: 10.2106/00004623-199308000-00009.

[13] MO F., AMOUX P.J., AVALLE M., SCATTINA A., SEMINO E., MASSON C., *Incidences of various passenger vehicle front-end designs on pedestrian lower limb injuries*, Int. J. Crashworthines, 2015, 20 (4), 337–347, DOI: 10.1080/13588265.2015.1012879.

[14] MO F.H., DUAN S.Y., JIANG X., XIAO S., XIAO Z., SHI W., WEI K., *Investigation of occupant lower extremity injures under various overlap frontal crashes*, Int. J. Auto Tech.-Kor., 2018, 19 (2), 301−312, DOI: 10.1007/s12239-018-0029-9.

[15] MO F., LI F., BEHR M., XIAO Z., ZHANG G., DU X., *A lower limb-pelvis finite element model with 3D active muscles*, Ann. Biomed. Eng., 2018, 46, 86–96, DOI: 10.1007/s10439-017-1942-1.

[16] MO F., LI J., DAN M., LIU T., BEHR M., *Implementation of controlling strategy in a biomechanical lower limb model with active muscles for coupling multibody dynamics and finite element analysis*, J. Biomech., 2019, 91, 51–60, DOI: 10.1016/j.jbiomech.2019.05.001.

[17] PEDEN M., SCURFIELD R., SLEET D., MOHAN D., HYDER A.A., JARAWAN E., MATHERS C., *Word report on road traffic injury prevention*, WHO, 2004.

[18] SAADÉ J., CUNY S., LABROUSSE M., SONG E., CHAUVEL C., CHRÉTIEN P., *Pedestrian injuries and vehicles-related risk factors in car-to-pedestrian frontal collisions*, Proceedings of the 2020 IRCOBI Conference Proceedings, Munich, IRCOBI, 2020, 278–289.

[19] TERESIŃSKI G., MADRO R., *Knee joint injuries as a reconstructive factors in car-to-pedestrian accidents*, Forensic. Sci. Int., 2001, 124 (1), 74–82, DOI: 10.1016/S0379-0738(01)00569-2.

[20] TIAN T., XIAO S., YOU S., ZHANG H., ZHANG L., MO F., *Effect of hip flexion angle on lower limb injuries of occupants in autonomous vehicle crashes*, Comput. Method Biomec., 2022, 1–14, DOI: 10.1080/10255842.2022.2162338.

[21] TOLEA B., ANTONYA C., BELES H., *Assessment of the injury severity of the pedestrian lower limbs at the collision with a vehicle*, Proc. of the Annual Session of Scientific papers "IMTOradea 2015", 2015, 14, 189–192, DOI: 10.15660/AUOFMTE.2015-1.13095.

[22] WANG B.Y., YANG J.K., OTTE D., WANG F., *Pedestrian lower extremity injury risk in car-pedestrian collisions*, Journal of Virbation and Shock, 2016, 35 (23), 1–5, DOI: 10.13465/j.cnki.jvs.2016.23.001.

[23] XIAO S., QIE Y., HUANG J., *Influence of restraint load on injury biomechanics in frontal impact based on dummy test*, IJST-T. Mech. Eng., 2020, 44, 1065–1075, DOI: 10.1007/s40997-019-00311-1.

[24] XIAO S., YOU S., TIAN T., WU J., ZHANG H., *Investigation of lower limb injury under different contact stiffness for drivers during frontal crash*, Acta Bioeng. Biomech., 2022, 24 (2), 83–93, DOI: 10.37190/ABB-02057-2022-02.

[25] YAN L., ZHANG W., CAO L., TANG J., DAI H., ZHANG K., *Design of centroid parameters of dummy heads models based on chinese anthropometric dimensions*, China Mechanical Engineering, 2018, 29 (07), 787–793, DOI: 10.3969/j.issn.1004-132X.2018.07.006.